

NUMERICAL AND PHYSICAL MODELLING OF MICROSTRUCTURE DEVELOPMENT DURING THE HOT ROLLING OF 30MnB4 STEEL ROUND BARS

LABER Konrad, DYJA Henryk, KAWAŁEK Anna, KOCZURKIEWICZ Bartosz

*Czestochowa University of Technology, Faculty of Production Engineering and Materials Technology,
Institute for Plastic Working and Safety Engineering, Czestochowa, Poland, EU*

Abstract

The paper presents the results of numerical and physical modelling of the development of microstructure during the process of hot rolling of 20 mm diameter plain round bars. The tests described in the paper were carried out for the technological conditions of a sample bar rolling mill. The material used for the tests was low-carbon cold heading steel, 30MnB4. The numerical modelling studies were carried out using the FORGE[®] and QTSteel programs. For the physical modelling of the process under examination, the metallurgical process simulator GLEEBLE 3800 was employed.

Keywords: Numerical modelling, physical modelling, microstructure development, cold upsetting steel

1. INTRODUCTION

Modelling of structural changes and, consequently, mechanical properties in the processes of thermomechanical treatment of metals and alloys is one of the most important research areas being the focus of the interest of scientific research centres concerned with materials engineering and plastic working [1, 2]. Using contemporary software programs relying on the finite element method, numerical modelling of thermomechanical treatment processes can be conducted [1, 3]. A complement to mathematical modelling, which enables complex problems encountered when developing new production processes to be solved with high efficiency, is the use of the physical simulation method [1]. In this study, finite element method-relying programs, FORGE[®] and QTSteel, were employed for the numerical modelling of the round bar hot rolling process. As a result of the numerical modelling using the FORGE[®] program, the distributions of rolled strip temperature, strain intensity and strain rate were determined, which were necessary for carrying out the modelling of microstructure development with the QTSteel program. The parameters determined from the numerical modelling with the FORGE[®] program provided also data for physical modelling using the simulator GLEEBLE 3800.

In the FORGE[®] program, the mechanical state of deformed material was described with the Norton-Hoff law [4].

$$S_{ij} = 2K_0(\varepsilon + \varepsilon_0)^{n_0} \cdot e^{(-\beta_0 T)} (\sqrt{3}\dot{\varepsilon})^{m_0-1} \dot{\varepsilon}_{ij} \quad (1)$$

where: S_{ij} - stress tensor deviator, $\dot{\varepsilon}$ - strain intensity rate, $\dot{\varepsilon}_{ij}$ - strain rate tensor, ε - strain intensity, ε_0 - initial strain, T - temperature, K_0 , m_0 , n_0 , β_0 - material constants related to the characteristic properties of the material concerned.

For the determination of the temperatures in the FORGE[®] program, a differential equation describing the temperature variations for unsteady heat transfer is used, which can be represented in the following form [4]:

$$\frac{\partial}{\partial x} \left(k_x \frac{\partial T_s}{\partial x} \right) + \frac{\partial}{\partial y} \left(k_y \frac{\partial T_s}{\partial y} \right) + \frac{\partial}{\partial z} \left(k_z \frac{\partial T_s}{\partial z} \right) + \left(Q - c_p \rho \frac{\partial T_s}{\partial t} \right) = 0 \quad (2)$$

where: k_x , k_y , k_z - functions of the distribution of thermal conductivity coefficients in the directions x, y, z; T_s - function describing the temperature; Q - function of the distribution of the deformation heat generation rate; c_p - function of the distribution of the specific heat; ρ - function of the distribution of metal density.

The QTSteel software used in the study for modelling of microstructure development makes it possible to predict the heat treatment response of through hardened carbon and alloy steels in terms of microstructure and mechanical properties [4]. Starting with the chemical composition and the austenitizing conditions of time and temperature, the software calculates the corresponding CCT diagram which describes the decomposition of the supercooled austenite into ferrite, pearlite, bainite and martensite [5]. The predicted or user-defined CCT diagrams can be used for computer simulation of the isothermal or non-isothermal transformation of the specified steel for the predefined cooling curve. The software divides the cooling curve into the sequences with a uniform cooling rate and calculates the percentage of various microstructural constituents for each sequence [5]. The computer simulation of austenite decomposition can then be followed by the simulation of tempering conditions (time, temperature), which will subsequently allow the calculation of the final mechanical properties [5].

The cooling rate (K/s) of a real cooling curve often deviates from the uniform rate. To describe the kinetics of transformation of the diffusion-controlled microstructural constituents X_i (ferrite, pearlite, bainite), the Avrami equation is applied; however, the values $k(T)$ and $n(T)$ are temperature-dependent during cooling with the dependence on the actual cooling rate [5]:

$$X_i(T, t) = (1 - \exp(-k(T) \cdot t^{n(T)})) \cdot X_\gamma \quad (3)$$

With regard to the calculation of martensite X_m , where the transformation is not time-dependent, but only temperature-dependent, the standard Koistinen-Marburg equation is used [5]:

$$X_m(T) = (1 - \exp(-b \cdot (T_{MS} - T)^n)) \cdot X_\gamma \quad (4)$$

The Vickers hardness is determined by multiple regression analysis for the following function [5]:

$$HV = C_0 + \sum(C1_i \cdot c_i \cdot \%Fe) + \sum(C2_i \cdot c_i \cdot \%Pe) + \sum(C3_i \cdot c_i \cdot \%Ba) + \sum(C4_i \cdot c_i \cdot \%Ma) \quad (5)$$

where: $C_0, C1, C2, C3, C4$ - regression coefficients, $c(i)$ - percentages of alloying additions, Fe, Pe, Ba, Ma - percentages of ferrite, bainite and martensite, respectively.

The calculation of the ultimate tensile strength R_m is based on the direct dependence of R_m on the HV-hardness (6). The calculation of the yield stress R_e is based on the general equation (7) [5]:

$$R_m = f(HV) \quad (6)$$

$$R_e = f(D_\alpha, CR, \sum(Fe, Pe, Ba, Ma)) \quad (7)$$

where: D_α - ferrite grain size, CR - average cooling rate (K/s), Fe, Pe, Ba, Ma - percentages of ferrite, bainite and martensite, respectively.

1.1. The aim, scope and methodology of the research

The main aim of the undertaken investigations was to compare the results of numerical modelling of microstructure development during the round bar hot rolling process (using the QTSteel program) with the physical modelling results obtained with the use of the GLEEBLE 3800 simulator. The investigations were carried out for the process of rolling 30MnB4 steel 20 mm-diameter round plain bars under the conditions of a sample continuous rolling mill.

At the first stage of the investigations, numerical modelling was performed using the FORGE[®] program. The determined parameters (the distributions of temperature, strain intensity, strain rate) were used as input data for the modelling of structure development using the QTSteel program and for the physical modelling of the rolling process under examination.

The results of the microstructure development numerical modelling included diagrams of austenite grain size variations in individual rolling passes and the distributions of hardness, yield point and tensile strength on the cross-section of finished bar.

At the next investigation stage, physical modelling of the examined process was carried out using the GLEEBLE 3800 simulator. From the material after the physical modelling, samples were taken for hardness tests and metallographic examinations.

At the final investigation stage, the results obtained from the numerical modelling were compared with those obtained from the physical modelling of the process under investigation.

2. ANALYSIS OF THE INVESTIGATION RESULTS

Chemical composition of the investigated material is given in **Table 1**.

Table 1 Chemical composition of 30MnB4 steel

Component contents [%]									
C	Mn	Si	P	S	Cr	Ni	Cu	Al	Mo
0.31	1.06	0.23	0.013	0.007	0.22	0.07	0.16	0.025	0.012
N	Pb	Al _{met}	As	Cb	V	Ti	B	Zn	Sn
0.0119	0.001	0.025	0.008	0.002	0.005	0.047	0.0030	0.018	0.013

The rheological properties of the material necessary for numerical modelling were determined in study [6]. The following boundary conditions were adopted for the numerical modelling: roll temperature, 60 °C; ambient temperature, 20 °C; the coefficient of heat exchange between the strip and the rolls, 3000 W / m²K; the coefficient of heat exchange between the strip and the air, 100 W / m²K; friction coefficient, 0.4; and friction factor, 0.8. The deformation process parameters for all rolling passes are summarized in **Table 2**. Break durations were assumed based on industrial data. After the final deformation, the material was cooled down to a temperature of 500°C, at a cooling rate of 5 °C / s, and then to 200 °C at 1 °C / s.

Table 2 Deformation parameters during the modelling of 30MnB4 steel round bar rolling

Pass No.	Deformation temperature, T [°C]	Strain, ε [-]	Strain rate, $\dot{\varepsilon}$ [1/s]	Interpass time, t [s]
1	1086	0.12	0.16	26.47
2	1057	0.39	0.35	19.89
3	1037	0.28	0.39	29.98
4	1023	0.59	0.96	11.33
5	1010	0.46	1.15	8.91
6	999	0.50	2.02	6.13
7	998	0.45	2.45	11.65
8	1005	0.48	4.71	3.35
9	1009	0.44	5.57	2.62
10	1022	0.54	10.39	1.85
11	1030	0.48	12.07	3.09
12	1049	0.50	20.53	2.28
13	1052	0.51	24.74	3.18
14	1069	0.50	46.34	1.35
15	1072	0.41	47.13	1.11
16	1087	0.51	79.93	0.90
17	1091	0.34	70.63	-

Sample results for rolling pass 1 are shown in **Figure 1**.

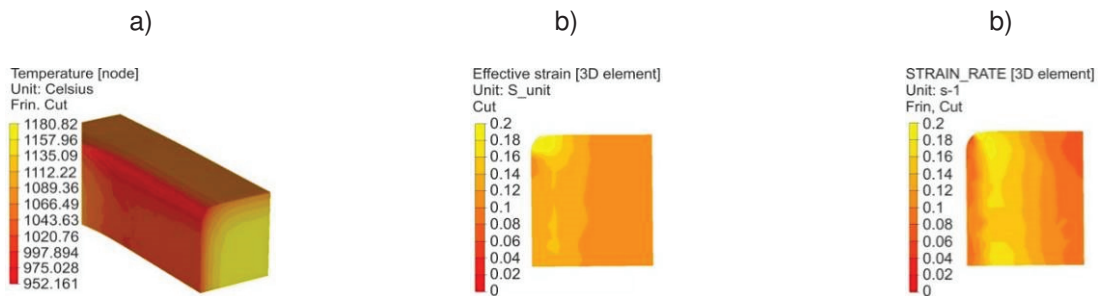


Figure 1 Distribution of temperature (a), strain intensity (b) and strain rate (c) during rolling of 30MnB4 steel in the first rolling stand

To increase the computation accuracy of the microstructure development modelling, the chemical composition and the actual CTP_c diagram of the investigated steel were implemented in the QTSteel program's database.

Figure 2 illustrates variations in 30MnB4 steel austenite grain size in successive passes of the continuous rolling line. The distributions of hardness and mechanical properties in the cross-section (slice) of 30 mm-diameter round bar, as computed with the QTSteel program in accordance with the preset deformation and cooling conditions, are shown in **Figure 3**.

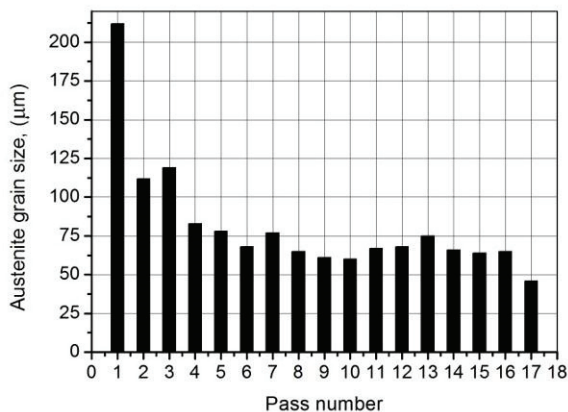


Figure 2 Variations in the austenite grain size of 30MnB4 steel in the 20 mm diameter round bar hot rolling process

The initial 30MnB4 steel austenite grain size was 200 μm. As the data in **Figure 2** shows, the austenite grain size decreased gradually as a result of the rolling process to attain a value of approx. 46 μm in the last rolling pass. In the first pass, the magnitude of deformation was too small for recrystallization to start, and the austenite grain had grown due to the long post-deformation break duration. A slight increase in the austenite grain size of the investigated steel was observed (in rolling passes: 3, 7, 11-13, 16). The analysis of the recorded plastic flow curves [6] showed that it was caused by the absence of recrystallization due to the too low deformation value, which was smaller than the critical value necessary for starting the softening processes, while in the case of exceeding this value - the too short duration of the inter-deformation break.

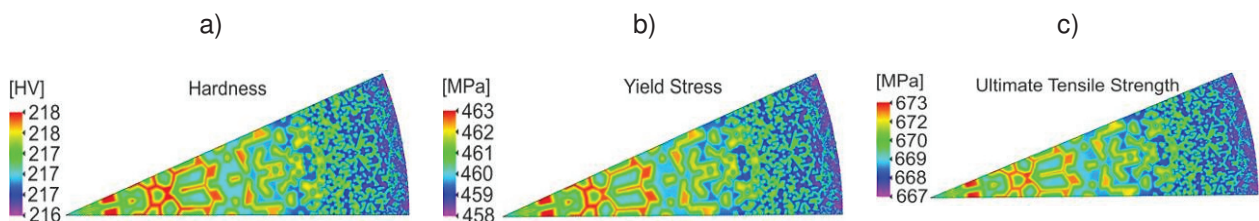


Figure 3 Distribution of hardness (a), yield point (b) and the ultimate tensile strength (c) on the cross-section of 30MnB4 steel round bar

From the numerical modelling results it was found that the average hardness value on the cross-section of finished bar amounted to approx. 217 HV. The average value of yield point R_e was about 460 MPa, while average ultimate tensile strength R_m , about 669 MPa.

The percentage fractions of individual microstructure constituents, as calculated with the QTSteel program, are shown in **Figure 4**.



Figure 4 The percentage fraction of ferrite (a) and pearlite (b) of the 30MnB4 steel bar cross-section

The data in **Figure 4** shows that the fraction of individual microstructure constituents of the finished bar after the cooling process was approx. 40% for ferrite and approx. 60% for pearlite.

The schematic diagram of heat treatment during the physical modelling of the bar rolling process using the GLEEBLE 3800 simulator is shown in **Figure 5**. The variations of the yield stress of the investigated steel grade and temperature during the physical modelling of the of bar rolling process in the uniaxial hot compression test are illustrated in **Figure 6**.

During physical modelling, only the last 3 deformations of the rolling line were modelled, assuming that the formation of the microstructure of the finished product takes place in the final rolling stage. This was confirmed by investigations carried out e.g. in study [7].

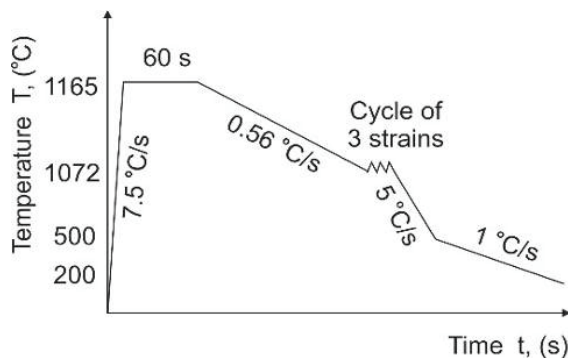


Figure 5 A schematic diagram of heat treatment during the physical modelling of the 20 mm-diameter plain round bar rolling process

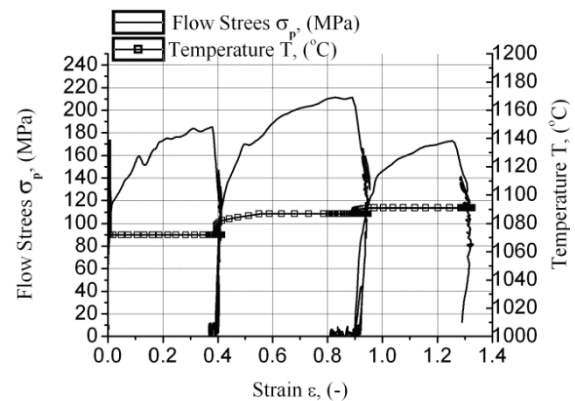


Figure 6 Variations in the yield stress and temperature of steel 30MnB4 during physical modelling

When analyzing the data in **Figure 6** it can be noticed that no softening had occurred after the first deformation, which manifested itself in an increase in yield stress. From the analysis of the plastic flow curves described in reference [6] it can be found that, for the analyzed deformation parameters, the leading phenomenon removing the hardening effects is dynamic recrystallization. In the case under analysis, none of the deformations exceeded the critical value for initiating dynamic recrystallization, therefore static recrystallization occurred. Unfortunately, the break duration of 1 s turned out to be too short, as a consequence of which a strengthening of the material resulted, which was visible in the form of an increasing stress value during deformation (the second deformation). In the subsequent pass (the third deformation), a strain accumulation occurred and dynamic recrystallization started, resulting in the refinement of the austenite grains.

An example of material microstructure after physical modelling is shown in **Figure 7**. The hardness values and the magnitudes of the yield point and ultimate tensile strength of the material after physical modelling, calculated on their basis, are given in **Table 3**.

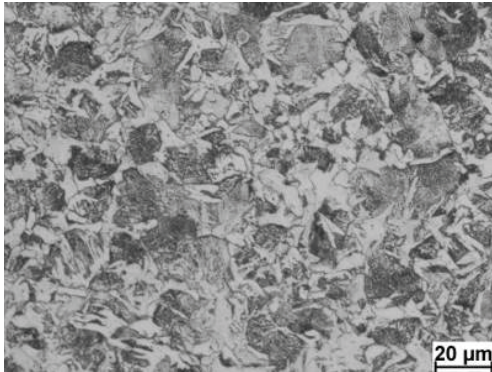


Figure 7 Microstructure of steel 30MnB4 after physical modelling

Table 3 Selected properties of steel 30MnB4 after the physical modelling of the 20-diameter round bar rolling process

Hardness [HV]	Yield point, R _e [MPa]	Ultimate tensile strength, R _m [MPa]
217.83	453.26	688.83

Based on the analysis of the data in **Figure 7** it can be found that the material after physical modelling had a fine-grained pearlitic-ferritic microstructure. The analysis of the microstructure of the investigated steel has shown that the fraction of individual microstructure constituents (pearlite and ferrite) is similar to the results obtained from the numerical modelling.

The differences between the hardness, yield point and ultimate tensile strength values obtained from the numerical modelling and the corresponding values obtained from the physical modelling were: approx. 0.4 % for hardness, approx. 1.5 % for the yield point, and approx. 2.9 % for the ultimate tensile strength.

The physical modelling method employed in the study, which involves the determination of the deformation parameters and temperature variations by numerical modelling followed by physical modelling of the process using the Gleeble 3800 simulator, has represented the phenomena occurring in the material during the actual rolling process with a good approximation, as confirmed by investigation results reported, e.g., in study [9]. On this basis it can be stated that numerical modelling of microstructure development using the QTSteel program, too, enables one to forecast the development of microstructure during the actual rolling process at high accuracy, and, as a result, to predict at high accuracy the mechanical properties examined in the study.

3. CONCLUSIONS

Based on the results of numerical and physical modelling of the development of microstructure during rolling of round bars of steel 30MnB4, the following conclusions have been drawn:

- the slight austenite grain size increase, observed in some rolling passes, is caused by the absence of recrystallization due to too low a deformation value (below the critical value, while in the case of exceeding this value - the too short duration of the break between successive deformations;
- from the numerical and physical modelling results it can be found that after the deformation and cooling process the finished bar had a pearlitic-ferritic microstructure, and the numerically computed fraction of microstructure constituents was approx. 60 % of pearlite and approx. 40 % of ferrite;
- from the results of the numerical modelling of the rolling process it can be inferred that, in the examined case, none of the deformations exceeded the critical value for initiation of dynamic recrystallization, and the softening took place as a result of static recrystallization;
- in the process under examination, the duration of breaks between final deformations of 1 second was too short for the complete static recrystallization, as a consequence of which a strengthening of the

material occurred in successive rolling passes up to the strain accumulation and the attainment of the critical value for dynamic recrystallization initiation, resulting in a slight decrease in the yield stress of the investigated steel grade in the last pass;

- the hardness, yield point and ultimate tensile strength values obtained from the numerical modelling correspond with high accuracy to the values obtained from the physical modelling; and
- the finite element method-relying QTSteel software program allows the structure development during the actual rolling process to be forecast with high accuracy and enables the mechanical properties of the examined steel grades to be accurately predicted.

ACKNOWLEDGEMENTS

This research work was financed from the resources of the National Research and Development Centre (Narodowe Centrum Badań i Rozwoju) in the years 2013-2016 as Applied Research Project No. PBS2/A5/0/2013.

REFERENCES

- [1] KUZIAK, R., PIETRZYK, M. Zastosowanie nowoczesnych metod modelowania matematycznego do optymalizacji procesu walcowania blach na gorąco. *Walcowanie i przetwórstwo blach i taśm*. [The use of modern mathematical modelling methods for the optimization of the plate hot rolling process. *Plate and strip rolling and processing*]. 18÷20.10.1995. Poraj. University Press of Czestochowa University of Technology, Czestochowa, 1995, p. 40.
- [2] SULIGA, M. The analysis of the mechanical properties of high carbon steel wires after multipass high speed drawing process in conventional and hydrodynamic dies, *Archives of Metallurgy and Materials*, Vol.59 No. 2, 2014, pp. 681-685.
- [3] SULIGA, M. Analysis of the heating of steel wires during high speed multipass drawing process, *Archives of Metallurgy and Materials*, Vol. 59 No.4, 2014, pp.1475-1480.
- [4] MRÓZ, S. *Proces walcowania prętów z wzdłużnym rozdzielaniem pasma* [The bar rolling process with longitudinal strip separation]. Series: Monografie no. 138. ISBN 978-83-7193-369-1. ISSN 0860-5017. University Press of Czestochowa University of Technology, Czestochowa 2008, p. 52.
- [5] QTSteel Software. *Metallurgical software for simulating the quench and tempering of steels*. User's Guide. Release 3.4.1 - including the rolling option. ITA-Technology and Software. MSL-Metaltech Services Ltd, 2015.
- [6] SAWICKI, S., DYJA, H., KAWAŁEK, A. Plastometric testing of rheological property of 20MnB4 and 30MnB4 micro-addition cold upsetting steels and C45 and C70 high carbon-steels. *International Scientific and Technical Conference Nanotechnologies of Functional Materials (NFM'2014)*. Sankt-Petersburg, 2014, pp. 67-72.
- [7] LABER, K., DYJA, H., KOCZURKIEWICZ, B., SAWICKI, S. Fizyczne modelowanie procesu walcowania walcówki ze stali 20MnB4 [Physical modelling of the 20MnB4 steel wire rod rolling process]. *The 6th Scientific Conference on ROLLING ENGINEERING 2014*. Ustroń, 2014, pp. 37-42.